

Frequency magnitude distribution and spatial correlation dimension of earthquakes in north-east Himalaya and adjacent regions

Ram Krishna Tiwari^{1,2*}, Harihar Paudyal²

¹ Central Department of Physics, Tribhuvan University, Kirtipur, Kathmandu, Nepal

² Birendra Multiple Campus, Tribhuvan University, Bharatpur, Chitwan, Nepal

* corresponding author, e-mail: ram.tiwari@bimc.tu.edu.np

Abstract

The north-east sector of the Himalaya is one of the most active tectonic belts, with complex geological and tectonic features. The b -value and spatial correlation dimension (D_c) of earthquake distribution in the north-east Himalaya and its adjacent regions (20–32°N and 88–98°E) are estimated in the present study. Based on seismicity and faulting pattern, the region is divided into five active regions, namely the (i) South-Tibet, (ii) Eastern-Syntaxis, (iii) Himalayan-Frontal Arc, (iv) Arakan-Yoma belt and (v) Shillong-Plateau. A homogeneous catalogue of 1,416 earthquakes ($m_b \geq 4.5$) has been prepared from a revised catalogue of the ISC (International Seismological Centre). The b -value has been appraised by the maximum likelihood estimation method, while D_c values have been calculated by the correlation integral method; b -values of 1.08 ± 0.09 , 1.13 ± 0.05 , 0.92 ± 0.05 , 1.00 ± 0.03 and 0.98 ± 0.08 have been computed for the South-Tibet, Eastern-Syntaxis, Himalayan-Frontal Arc, Arakan-Yoma belt and Shillong-Plateau region, respectively. The D_c values computed for the respective regions are 1.36 ± 0.02 , 1.74 ± 0.04 , 1.57 ± 0.01 , 1.8 ± 0.01 , and 1.83 ± 0.02 . These values are > 1.5 , except for the South-Tibet (1.36 ± 0.02). The b -values around the global average value (1.0) reflect the stress level and seismic activity of the regions, while high D_c values refer to the heterogeneity of the seismogenic sources.

Key words: North-east India, b -value, maximum likelihood estimation, correlation dimension

1. Introduction

With regard to time, space and size, earthquake occurrences own a power-law relation. The b -value (Gutenberg & Richter, 1944) and fractal dimension – D_c (Grassberger & Procaccia, 1983) are two scale-invariant exponents in earthquake data analysis that obey a power law relation. The spatio-temporal variations of these parameters have importance in our understanding of stress environments and features of seismogenic structures. The b -value is associated to variations in both local and regional stresses (Mogi, 1967; Scholz, 1968; Wiemer & Wyss, 1997; Khan & Chakraborty, 2007; Bora & Baruah, 2012;

El-Isa & Eaton, 2014; Mousavi, 2017a, b; Bora et al., 2018), types of faults (Ishibe et al., 2015) and creeping segment of the fault and asperity existing in the fault (Zhao & Wu, 2008), while the fractal dimension can be used to explain the complexity present in a ruptured surface (Kagan & Knopoff, 1978; Mandelbrot & Wheeler, 1983; Turcotte, 1989). The D_c in different zones may vary and the variation can be related to geo-structural heterogeneity (Aviles et al., 1987). The relation between the b -value and D_c has been studied widely during the last three decades (Hirata, 1989a; Öncel et al., 1996; Legrand, 2002; Wyss et al., 2004; Ghosal et al., 2012; Pailoplee & Choowong, 2014; Wu et al., 2017; Mondal et al., 2019; Chen & Zhu, 2020).

The Himalaya was created due to continuous convergence and under-thrusting of the Indian continental plate below the Eurasian plate. Its northern boundary is the Tibetan plateau; the southern boundary is the Indo-Gangetic plane. Here, we select the north-east Himalayan region, which is bounded by 20–32°N and 88–98°E, in order to study the fractal nature of earthquake distribution. This region includes Sikkim, Bhutan, north-east Himalaya, and its adjoining Tibet region, Arakan-Yoma belt and adjoining parts of Bangladesh and Myanmar (Fig. 1). It is characterised by a complex geological and tectonic setting with several thrusts, faults, folds and lineaments (Berthet et al., 2014; Dasgupta et al., 2021).

Having an intricate geotectonic setup, the seismicity of the region is remarkably high in which earthquakes with wide-range magnitude have been a common phenomenon since historical times (Angelier & Baruah, 2009; Bhattacharya et al., 2010; Zhang et al., 2012). The great Shillong earthquake of June 12, 1897 (Mw 8.0) was in the northern parts of the Shillong Plateau, while on August 15, 1950, the great Assam earthquake (Mw 8.6) occurred in

the Mishmi tectonic block (Kayal, 2010; Liu et al., 2015). These great earthquakes have made the region seismically very active (Bilham et al., 2017). The Kopili Fault zone, which separates the Shillong Plateau and the Mikir Massif (Fig. 1; Kayal et al., 2006, 2012) had earlier produced two strong earthquakes, i.e., in 1869 (Mw 7.7) Cachar earthquake (Nandy, 2005) and in 1943 (Mw 7.1) earthquake (Nandy & Dasgupta, 1991) and has the potential to experience strong earthquake in the future (Bora et al., 2013). The segment of the crust between the rupture zone of the Shillong and Assam earthquakes has been identified as a potential host of a future great earthquake (Khattari & Tyagi, 1983; Angelier & Baruah, 2009). In addition, the area bounded by the Dhubri-Chungthang fault (DCF) zone and the Main Himalayan Thrust (MHT) may potentially host M7 to M8 earthquakes (Fig. 1; Diehl et al., 2017).

Most earthquakes in the Himalaya are shallow and intermediate in focus and the major cause of these earthquakes is a shallow dipping-downward motion of the Indian plate under the Eurasian landmass (Molnar & Tapponnier, 1975; Kayal et al., 1993). Furthermore, the subducting Indo-Bur-

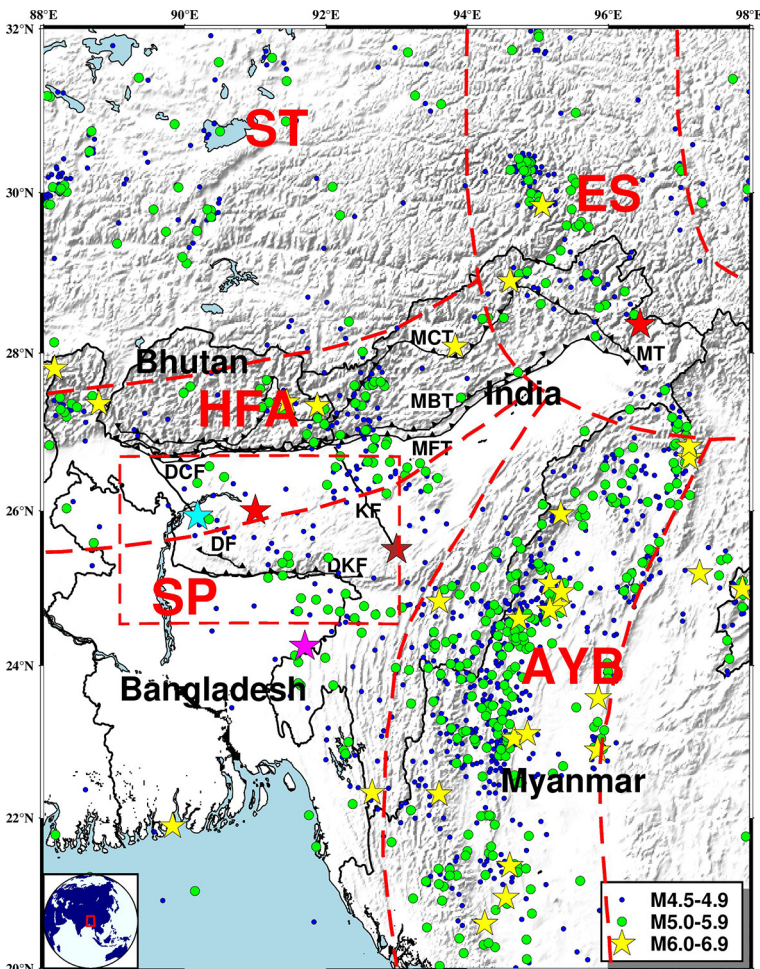


Fig. 1. Epicentral distribution of earthquakes ($M_c \geq 4.5$) in the study region. The yellow stars in different blocks stand for earthquakes (magnitude ≥ 6.0 mb). Regions are as follows: ST - South Tibet; ES - Eastern-Syntaxis; HFA - Himalayan-Frontal Arc; AYB - Arakan-Yoma belt; SP - Shillong-Plateau (Panthi et al., 2013). The red star in region ES stands for the 1950 Assam earthquake, while that inside the rectangular box signifies the 1897 Shillong earthquake. The cyan star is for the 1930 Dhubri earthquake, a brown star for the 1869 Cachar earthquake and a magenta star for the 1918 Srimangal earthquake. Abbreviations: MCT - Main Central Thrust; MBT - Main Boundary Thrust; MFT - Main Frontal Thrust; KF - Kopili Fault; MT - Mishmi Thrust; DCF - Dhubri-Chungthang Fault; DF - Dapsi Fault; DKF - Dauki Fault. The red box in the inset map at the bottom left-hand corner of the map depicts the study area in a global scenario.

ma Range (IBR) in the east is also responsible for a prominent level of seismic activity in the region (Verma et al., 1976; Thingbaijam et al., 2008; Bora et al., 2022a, b). From our study of the literature, the north-east Himalaya and its nearby regions are demarcated as a potential zone for strong seismic activity in the future. Therefore, the present study attempts to enhance our understanding of regional features of seismicity, stress level and crustal heterogeneity.

2. Seismicity of the region and division of seismic zones

A total of 22 large earthquakes with $M \geq 7$, including the Shillong earthquake of Mw 8.0 (1897) and Assam earthquake of Mw 8.6 (1950), have occurred in the north-east region between 1897 and 1962 (Kayal et al., 1993; Islam et al., 2011; Tandon & Gupta, 2020). Other notable events are the 1869 Cachar earthquake (Mw 7.7), the 1918 Srimangal earthquake (Mw 7.5) and the 1930 Dhubri (Mw 7.1) (see Raghu Kanth & Dash, 2010). The high seismicity of this region can also be understood from the fact that it has experienced 29 events (magnitude ≥ 6.0 mb) for the period 1964–2020. Thus, it can be inferred that a considerable amount of strain energy is stored along this part of the Himalaya and the regions divided are tectonically active.

The division of the study area into five regions (Fig. 1) is based on the seismic activity and nature of faulting (Panthi et al., 2013). These regions are the South-Tibet (ST), Eastern-Syntaxis (ES), Himalayan-Frontal Arc (HFA), Arakan-Yoma belt (AYB) and Shillong-Plateau (SP). The normal faulting pattern is predominant in South-Tibet. Eastern-Syntaxis is made up with both thrust fault and transverse faults. The Himalayan-Frontal Arc shows thrust faulting with predominant major faults such as the MCT (Main Central Thrust) and MBT (Main Boundary Thrust; Fig. 1). The Arakan-Yoma region has more complex tectonics compared to others, in which a near-equal percentage of normal and thrust faulting is established (Bora, 2016). The Shil-

long-Plateau shows a tectonically important pop-up structure induced by plate convergence (Islam et al., 2011). These five regions enclose only 1,347 earthquakes with the Arakan-Yoma belt having a large number of earthquakes (727) and the Shillong Plateau having fewer (83) (Table 1).

3. Compilation of a seismicity database and methodology

A comprehensive and reliable seismicity database covering a wide range of magnitudes is needed to draw meaningful inferences from seismicity studies. For the preparation of a homogeneous catalogue, we have used the revised earthquake catalogue of the International Seismological Centre, ISC (Bondár & Storchak, 2011; Storchak et al., 2017, 2020). We have retrieved 5,013 earthquakes having body wave magnitude (mb) for the region 20–32°N and 88–98°E between January 22, 1964 and May 25, 2020. The declustering of the catalogue has been performed by the linked-window method (Reasenber, 1985) in order to remove dependent events such as foreshocks and aftershocks. We have then retained 4,845 earthquakes whose completeness (M_c) has been checked for a time window of 20 years from the maximum curvature technique in ZMAP package (Wiemer, 2001). For the time window from 1964 to 1984, M_c has been found to be 4.8. The M_c is 4.0 for the time window from 1984 to 2004 and 3.8 for 2004 to 2020. Although the average value of M_c for these three time windows is 4.2, the best fitted line is obtained for a completeness magnitude $M_c \geq 4.5$ mb with a b-value of 1.01 ± 0.02 . Thus, the final analysis is best on earthquake data with completeness magnitude 4.5 mb (Fig. 2). The completeness magnitude of the prepared catalogue is in agreement with the completeness magnitude of the preceding work (Sarkar et al., 2020). The maximum curvature technique has been used for estimation of M_c and b-value, because it gives a stable result even for fewer events. Thus, it has an advantage over other techniques such as the b-value stability technique (Cao & Gao, 2002) and the entire

Table 1. Information on the number of earthquakes, duration, focal depth and magnitude range in the five regions studied. For location of the regions see Figure 1.

| Region | Number of earthquakes | Time period | Depth (km) | Magnitude (mb) |
|-----------------------------|-----------------------|-----------------------|-------------|----------------|
| South-Tibet (ST) | 124 | 1964/06/10–2020/01/29 | 2.30–101.90 | 4.5–6.5 |
| Eastern-Syntaxis (ES) | 247 | 1965/06/15–2020/02/01 | 3.60–51.00 | 4.5–6.1 |
| Himalayan-Frontal Arc (HFA) | 166 | 1964/02/18–2020/04/15 | 6.50–65.80 | 4.5–6.1 |
| Arakan-Yoma belt (AYB) | 727 | 1964/01/22–2020/05/25 | 6.10–84.70 | 4.5–6.9 |
| Shillong-Plateau (SP) | 83 | 1966/02/24–2020/04/05 | 1.70–50.20 | 4.5–5.9 |

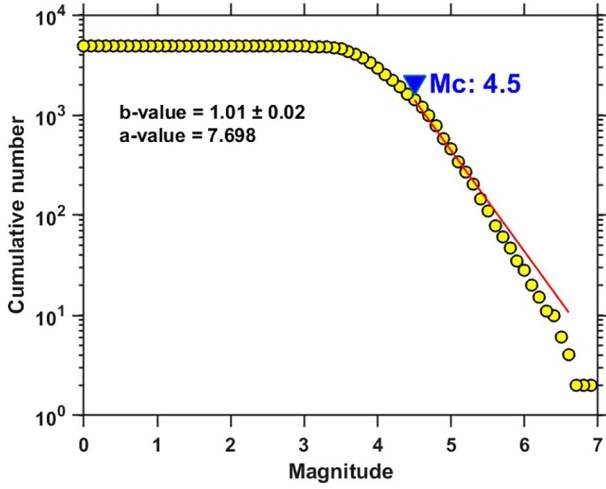


Fig. 2. b-value (1.01 ± 0.02) and magnitude of completeness ($M_c \geq 4.5$ mb) of dataset. The slope of the fitted red line gives the b-value.

magnitude range technique (Woessner, 2005). The database then contains 1,416 earthquakes covering the entire study region.

The power law relating magnitude of the earthquakes and their frequency of occurrence (Gutenberg & Richter, 1944; Nava et al., 2017) is:

$$\log N_e(M_e) = a - b(M_e - M_c); M_e \geq M_c \quad (1)$$

In equation (1), N_e is the numeral of earthquakes with magnitude M_e with $M_e \geq M_c$. The constant 'a' is the intercept on the y axis which depends on the region and timeframe of the study and describes the seismic assembly (El-Isa & Eaton, 2014). The other constant b is the slope of the linearly fitted line, also known as b-value, which gives the relative number of small to large earthquakes (Nava et al., 2017). A high value of b means that the fraction of smaller events is large and a low value of b means that the fraction of larger events is greater. It has an inverse relation with the stress level of the region (Ghosal et al., 2012; Scholz, 2015), and many studies have found a drop in the b-value prior to large earthquakes, tailed by an increase in the b-value after the main shock (Wiemer & Wyss, 1997, 2000; Pudi et al., 2020).

Table 2. Magnitude of completeness (M_c), a-value, frequency magnitude distribution b-value, correlation dimension (D_c) and coefficient of determination (R^2) of the regions studied. For location of the regions see Figure 1.

| Region | M_c | a-value | b-value | D_c | R^2 for D_c |
|-----------------------------|-------|---------|-----------------|-----------------|-----------------|
| South-Tibet (ST) | 4.5 | 6.150 | 1.08 ± 0.09 | 1.36 ± 0.02 | 0.997 |
| Eastern-Syntaxis (ES) | 4.5 | 7.482 | 1.13 ± 0.05 | 1.74 ± 0.04 | 0.997 |
| Himalayan-Frontal Arc (HFA) | 4.5 | 6.363 | 0.92 ± 0.05 | 1.57 ± 0.01 | 0.999 |
| Arakan-Yoma belt (AYB) | 4.5 | 7.374 | 1.00 ± 0.03 | 1.80 ± 0.01 | 0.988 |
| Shillong-Plateau (SP) | 4.5 | 6.333 | 0.98 ± 0.08 | 1.83 ± 0.02 | 0.996 |

The b-value in the present study is estimated by the maximum likelihood method (Aki, 1965):

$$b = \frac{\log_{10} e}{\bar{M} - (M_c - \frac{\Delta M_c}{2})} \quad (2)$$

In equation (2), \bar{M} is the average value of the magnitudes, M_c is minimum magnitude of the sample and ΔM_c is the binning thickness of the data considered. The standard error (Δb) on the value of b is estimated by (Shi & Bolt, 1982):

$$\Delta b = 2.30 \times b^2 \sqrt{\sum_{i=1}^{n_e} \frac{(M_i - M_c)^2}{n_e(n_e - 1)}} \quad (3)$$

In equation (3), n_e is the total number of earthquakes in a sample window. For all five regions considered the standard errors, $\Delta b \leq 0.09$, confirm fewer uncertainties in the evaluation of the b-value (Table 2).

The correlation dimension is obtained from the correlation integral method (Grassberger & Procaccia, 1983) in which the correlation function is defined as:

$$C(r) = \frac{2}{N_c(N_c - 1)} \sum_i^{N_c} \sum_{i \neq j}^{N_c} H(r - r_{ij}). \quad (4)$$

In equation (4), N_c is the total number of earthquakes in the window considered, $H(r - r_{ij})$ is the Heaviside step function, r is the scaling radius, and r_{ij} is the distance between the two epicentres determined by the spherical triangle method (Hirata, 1989a, 1989b) by the formula:

$$r_{ij} = \cos^{-1}(\cos \theta_i \cos \theta_j + \sin \theta_i \sin \theta_j \cos(\phi_i - \phi_j)) \quad (5)$$

Where θ_i and θ_j are the latitudes, while ϕ_i and ϕ_j are the longitudes of the epicentres of the earthquake. The arc distance between the two epicentres (θ_i, ϕ_i) and (θ_j, ϕ_j) is then obtained by multiplying r_{ij} with the radius of the earth. The correlation integral is related to the correlation dimension by the power law in the scaling region as:

$$C(r) = r^D \quad (6)$$

The scaling region of is selected between the saturation and depopulation limits (Nerenberg & Essex, 1990). The slope of fitted straight line in the linear part of the plot between $\log C(r)$ and $\log(r)$ estimates the correlation dimension as

$$D_c = \lim_{r \rightarrow 0} \frac{\log C(r)}{\log(r)} \quad (7)$$

The uncertainty in calculation of correlation dimension (root mean square error) is estimated by the formula:

$$RMSE = \sqrt{\frac{(P_i - O_i)^2}{n}} \quad (8)$$

where is P_i the i^{th} predicted value and O_i is the i^{th} observed value and n is the number of observations. The uncertainty in $D_c \leq 0.04$ indicates fewer uncertainties in the estimation of fractal dimension (Table 2).

The seismic moment curve shows two jumps in the years 1988 and 2016, releasing 0.79×10^{20} Nm and 1.83×10^{20} Nm energy, respectively, from the study region (Fig. 3). The range of the seismic moment (0.54 – 0.79) $\times 10^{20}$ Nm may be attributed to a seismic energy release after the Indo-Burma earthquake on August 6, 1988 (Mw 7.2) (Devi et al., 2021), while the range (1.57 – 1.83) $\times 10^{20}$ Nm may be attributed to the seismic energy release after the Manipur earthquake on January 3, 2016 (Mw 6.7) (Fig. 3; Borgohain et al., 2018). These values are comparable with the seismic moment estimated from the spectral analysis of P-waves of 162 local

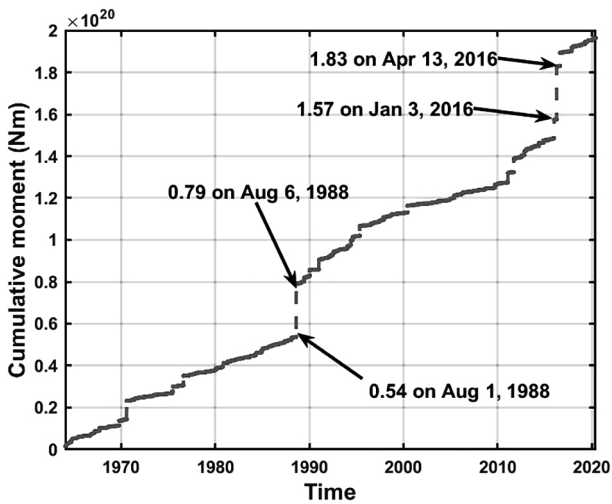


Fig. 3. Seismic moment release curve showing quick jumps in 1988 and 2016.

earthquakes in the Shillong-Mikir Hills plateau and its adjoining region in north-east India (Bora et al., 2013; Bora, 2016).

4. Results and discussion

4.1. b-value and earthquake occurrences

The frequency of earthquake occurrences in the five regions are explained on the basis of seismic a-values and b-values. The b-value ranges from 0.92 to 1.13 for these regions. The lowest b-value 0.92 ± 0.05 has been computed for the Himalayan-Frontal Arc region, while the highest value 1.13 ± 0.05 is seen for the Eastern-Syntaxis region. The b-value is 1.08 ± 0.09 for the South-Tibet, 1.00 ± 0.03 for the Arakan-Yoma belt and 0.98 ± 0.08 for the Shillong-Plateau (Fig. 4; Table 2).

The b-values obtained for these regions are close to the global mean value of 1.0. This indicates that the regions selected are seismically active. The observed a-values and b-values for the South-Tibet (6.15 and 1.08 ± 0.09), Eastern-Syntaxis (7.48 and 1.13 ± 0.05) and Arakan-Yoma belt (7.37 and 1.00 ± 0.03) reflect the high seismic activity due to the increment of heterogeneity in the crust (Khan et al., 2011; Akol & Bekler, 2013). The crustal heterogeneity may be linked to deformation on the crust caused by folding, faulting and cracking of the rock. The relatively low b-values 0.92 ± 0.05 and 0.98 ± 0.08 observed for the Himalayan-Frontal Arc and the Shillong Plateau (Fig. 4; Table 2) may indicate the accumulation of stress caused by the tectonic interaction between these landmasses (Panthi et al., 2013; Bora, 2016).

The temporal variation of the b-value has been determined for the five selected regions. For the South-Tibet region, a small increment in the b-value is noted from 1.15 to 1.22 during the study period (Fig. 5a). The gradual decrease in the b-value from 2.52 to 1.30 is seen for the Eastern-Syntaxis region (Fig. 5b), while the Himalayan-Frontal Arc (Fig. 5c) demonstrates a rise in the b-value from 1.36 to 1.61 and then a falls down to 1.37. An oscillating nature of variation in the b-value is noted for the Arakan-Yoma belt (Fig. 5d), between ~ 1.5 to ~ 1.1 for the study period. Finally, for the Shillong-Plateau, the b-value rises from 1.11 to 1.20 and then falls to 1.10 (Fig. 5e). The lowering trend of the b-value for the Eastern-Syntaxis may be the cause of the earthquakes of similar magnitude in the region and suggests an accumulation of stress in the region. The oscillating variation for the Arakan-Yoma belt indi-

cates continuous accumulation and release of stress in the region through small to moderate earthquakes. A similar type of variation in the b-value was also recorded for north-east India during 1975 to 2015 by Kumar & Sharma (2019).

From the b-value contour map of the region (Fig. 6), it is inferred that the seismic b-values obtained are evenly distributed over the entire region and dominated by b-values of ≤ 1.0 . Relatively low

b-value contours (0.8–0.9) have been obtained along the Dhubri-Chungthang Fault (DCF) zone in the Himalayan-Frontal Arc region (HFA), the Dapsi Fault (DF) zone, the Dauki Fault (DKF) zone and the Kopili Fault (KF) zone in the Shillong Plateau region (SP). Furthermore, b-value contours (0.9) have been obtained along the Mishimi Thrust (MT) zone in the Eastern-Syntaxis region (ES). Relatively high b-value contours (1.1–1.2) have been found for

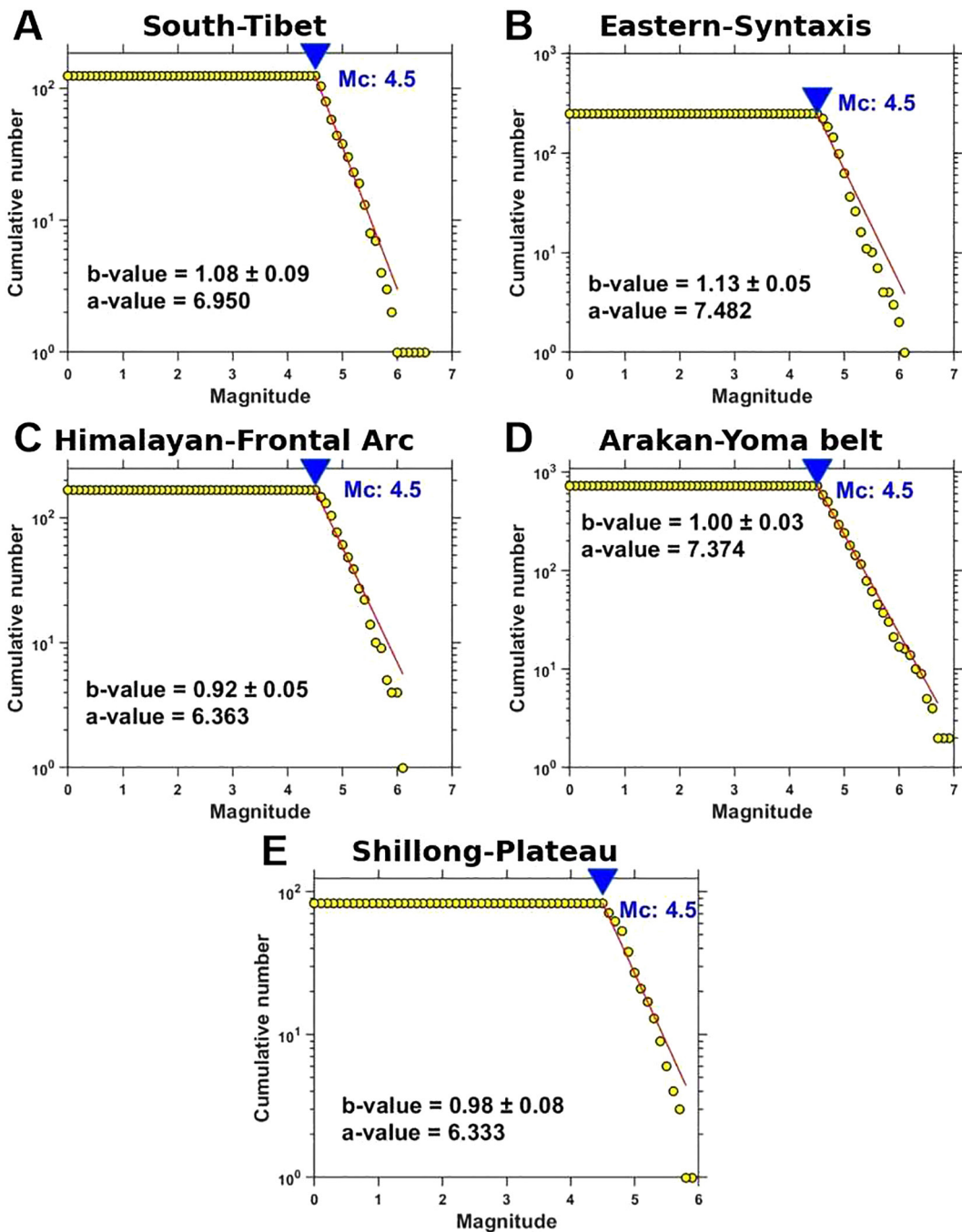


Fig. 4. Magnitude-frequency plots computed from the maximum likelihood solution for selected regions. For location of the regions see Figure 1.

the latitude 22–24°N and longitude 92.5–95°E in the Arakan-Yoma belt region (AYB; Fig. 6). The higher b-values may be due to reciprocated interaction between the Shillong Plateau, Mikir Hills, Kopili Fault zone and the IBR (Khan et al., 2011).

In earlier papers, b-values were observed to be in the range 0.6 to 1.0 and in particular, higher b-value contours were mapped for the Shillong Pla-

teau (Bhattacharya & Kayal, 2003), b-values from 0.6 to 1.0 were also computed for the same region (Bhattacharya et al., 2010). Thus, the b-values estimated in the present work are in agreement with previous publications. Some researchers have also found b-value variations from 0.75 to 1.54 for the Indo-Burma range – IBR (Bora et al., 2018).

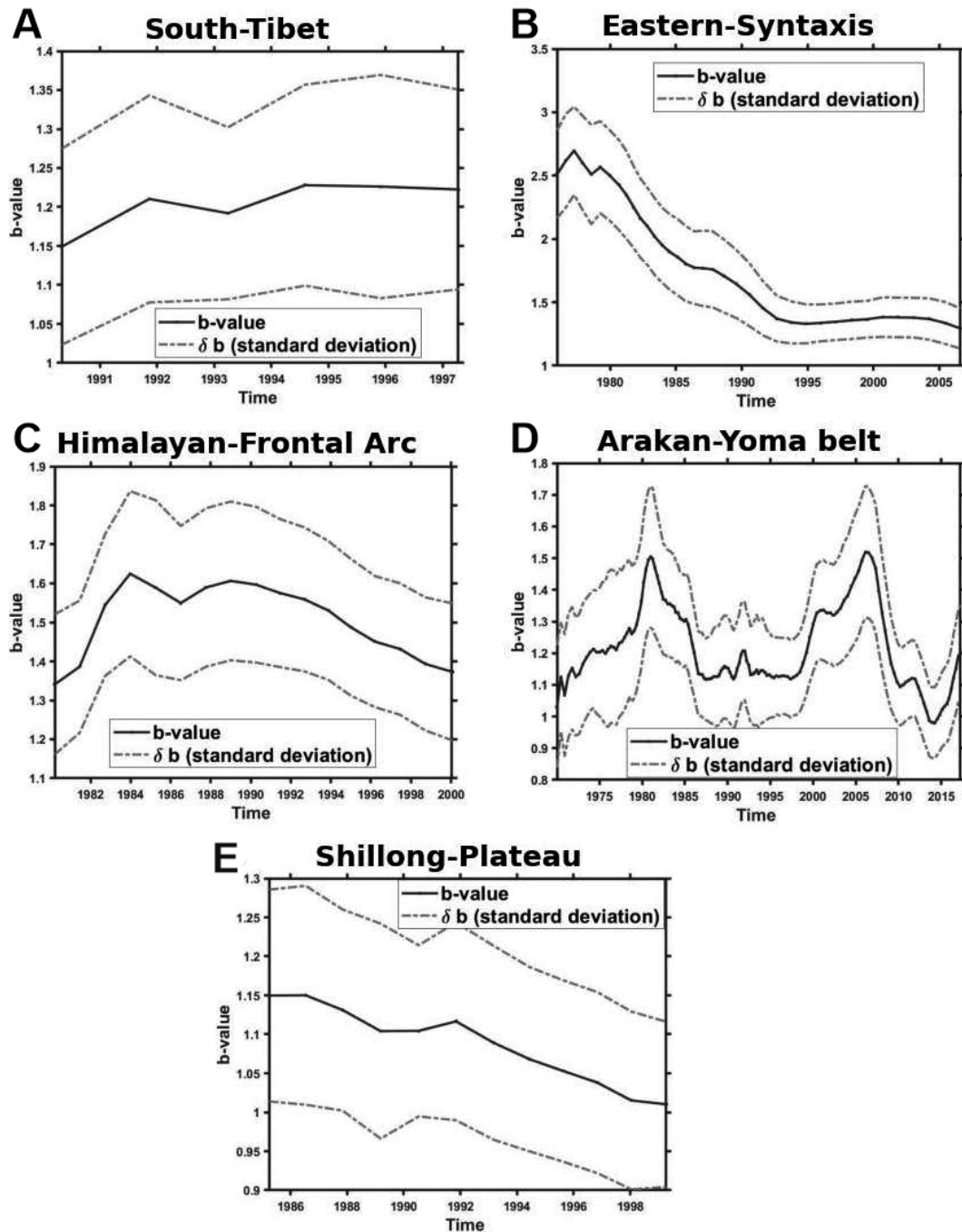


Fig. 5. b-value variation with time for selected regions. The temporal variation of the b-value is studied for a window size of 100 events with an overlap of 4%, except for the Shillong-Plateau region where a window size of only 60 events is taken because of paucity of data. For location of the regions see Figure 1.

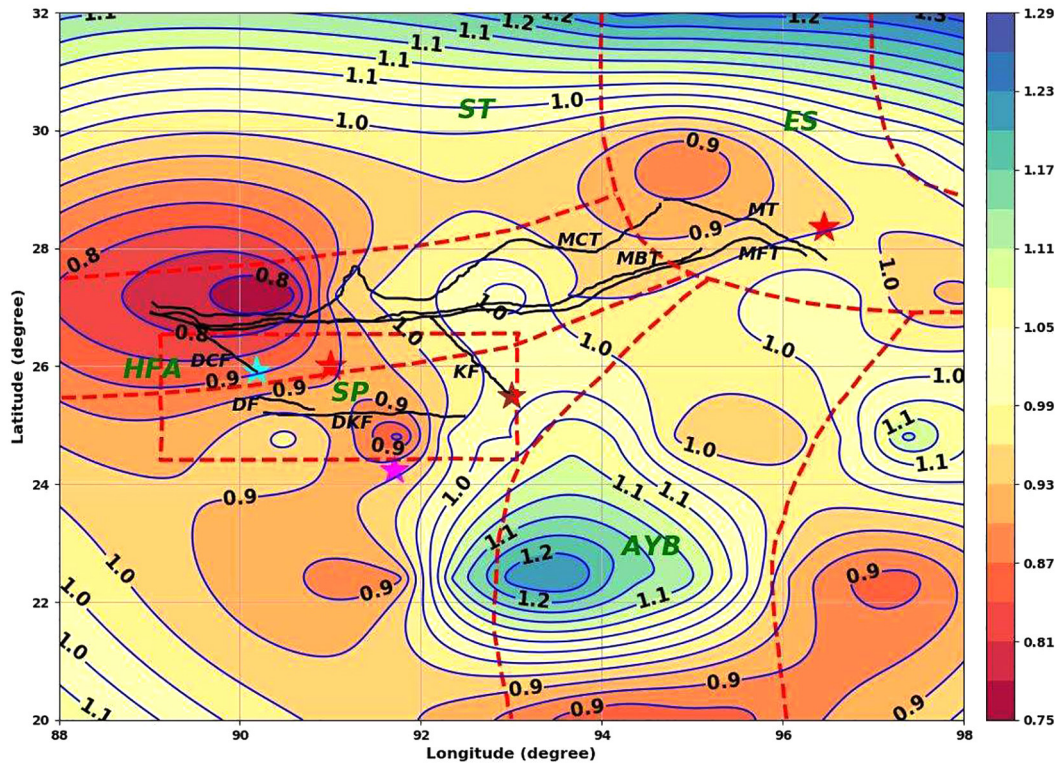


Fig. 6. The contour map of b-values in the study area. The b-values are plotted for the mean value of longitude and latitude of $2^\circ \times 2^\circ$ square grids with window shifting of 0.5° along the direction of longitude. For detailed explanations and location of the regions see Figure 1.

4.2. Fractal correlation dimension of spatial distribution of epicentres

The correlation dimension (D_c) for different regions can be found in Table 2 and D_c value graphs in Figure 7. The correlation dimension obtained for the South-Tibet region is 1.36 ± 0.02 . It is 1.74 ± 0.04 for the Eastern-Syntaxis, 1.57 ± 0.01 for the Himalayan Frontal Arc, 1.80 ± 0.01 for the Arakan-Yoma belt and 1.83 ± 0.02 for the Shillong-Plateau. The high D_c value along the Shillong-Plateau (1.83) is followed by the value 1.80 for the Arakan-Yoma belt, while the lowest value (1.36) is noted for the South-Tibet (Fig. 7; Table 2). The D_c value of seismically dynamic sources ranges between 0 and 2 (Tosi, 1998) and a value close to 2 is a sign of the distribution of events over a two-dimensional fault plane (Yadav et al., 2011; Ghosal et al., 2012). Also, the degree of clustering of earthquakes is inversely proportional to the fractal dimension, that is, a high value is associated with a low clustering and vice versa (Hirata, 1989a; Roy & Padhi, 2007; Roy et al., 2015). Therefore, the region under study, with a fractal dimension 1.36–1.83, shows near-plane characteristics of seismogenic structures, where earthquakes are densely distributed. In particular, the Shillong-Pla-

teau ($D_c = 1.83 \pm 0.02$) and the Arakan-Yoma belt with ($D_c = 1.80 \pm 0.01$) indicate a near-planar nature of seismogenic structures and the D_c value < 1.5 for South-Tibet indicates an active linear fault system in the region (Yadav et al., 2011). Although, the D_c value obtained in the present study are higher than results of earlier workers (0.8 to 1.2) for eastern Himalaya and southern Tibet (Singh et al., 2009) these results agree with the D_c value range (0.37 to 1.81) obtained by Sarkar et al. (2020).

The contour map (Fig. 8) shows both low D_c contours (~ 1.1) and high D_c contours (~ 1.9). Comparatively low D_c (1.1–1.5) contours are noted in the South-Tibet region (ST; see Fig. 1) while an intermediate values of D_c contour (1.2–1.6) are seen in the Eastern-Syntaxis region (ES). In addition, D_c contours of a high range from 1.5 to 1.6 are also noted along the Mishimi Thrust (MT) zone in the Eastern-Syntaxis region. High D_c contours (1.8–1.9) are demonstrated in the Himalayan-Frontal Arc region (HFA), and Shillong Plateau region (SP), accommodating underlined faults DCF, DF, KF, and DKF (Fig. 8; Table 2). Moreover, high D_c contours (1.6–1.8) are also seen for the Arakan-Yoma belt (AYB). These results indicate the gathering of epicentres around a two-dimensional space. This ultimately reduces the stress-bearing capacity of the rocks, making the

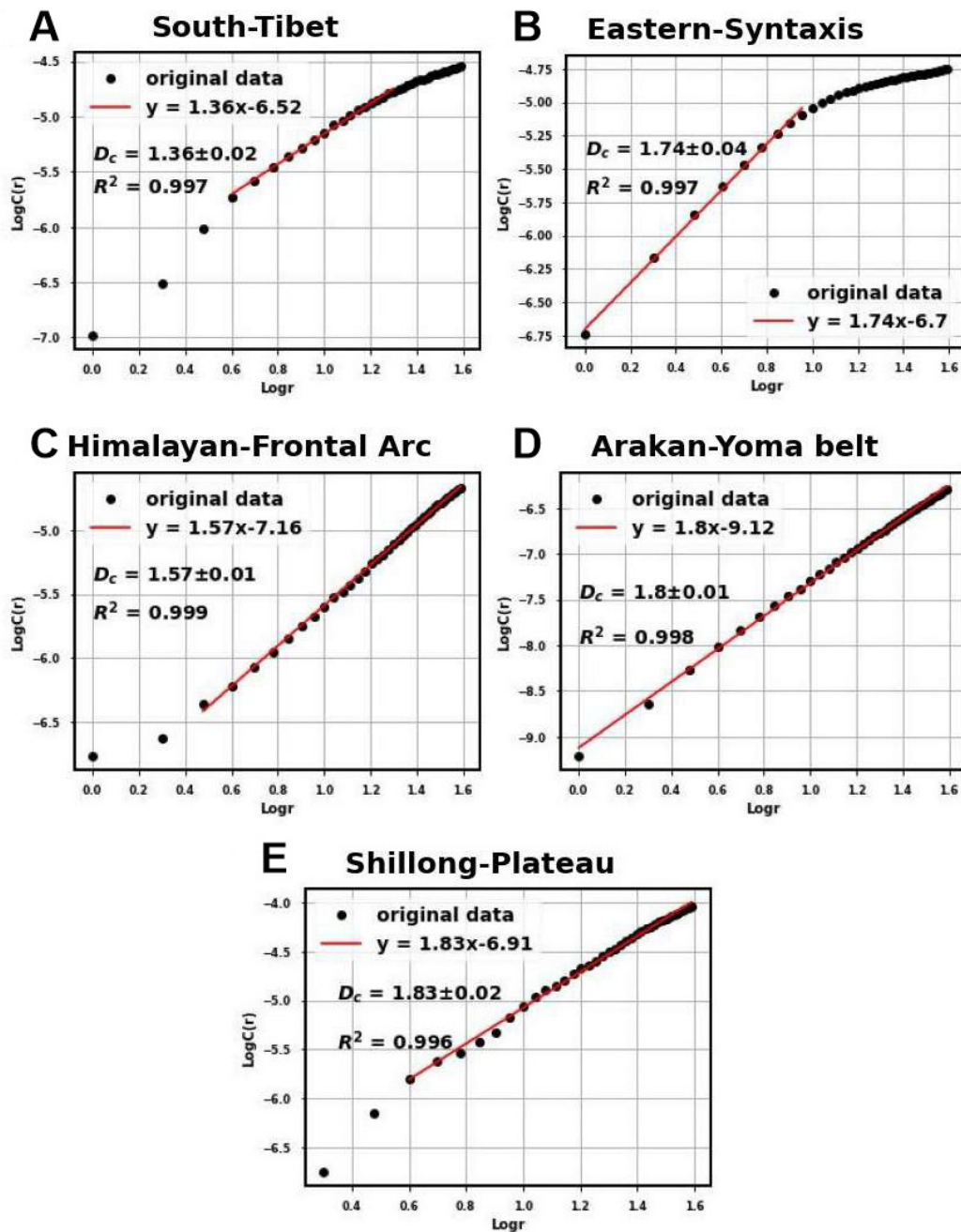


Fig. 7. The plot of $\text{Log}C(r)$ vs $\text{Log}r$ for five selected regions under study. The C in $\text{Log}C$ along y-axis is the correlation integral function, while r in $\text{Log}r$ along x-axis is the scaling radius. The slope of the linear part of the plot estimates the fractal dimension D_c . For location of the regions see Figure 1.

crustal surface heterogeneous. A heterogeneous crustal structure is responsible for a heterogeneous stress field that makes the region favourable for the growth of a tremor.

The interrelationship between D_c and b -value has been calculated for different regions of the world. A positive co-relationship between them was proposed for intermediate events with $D_c = 2b$ (Aki, 1965), which is supported by studies carried out in the south-eastern Iran-Bam region (Roy &

Padhi, 2007) and in İzmit, Turkey (Oncel & Wilson, 2002, 2007). The negative co-relationship reported by Hirata (1989b) between two scaling exponents has also been supported by a study carried out in the north Anatolian fault zone (Öncel et al., 1995, 1996). As far as the present study is concerned, no correlation has been found between D_c and b -value as depicted by the correlation function $D_c = -0.08b + 1.6$ and $R^2 = 0.002$ (Fig. 9).

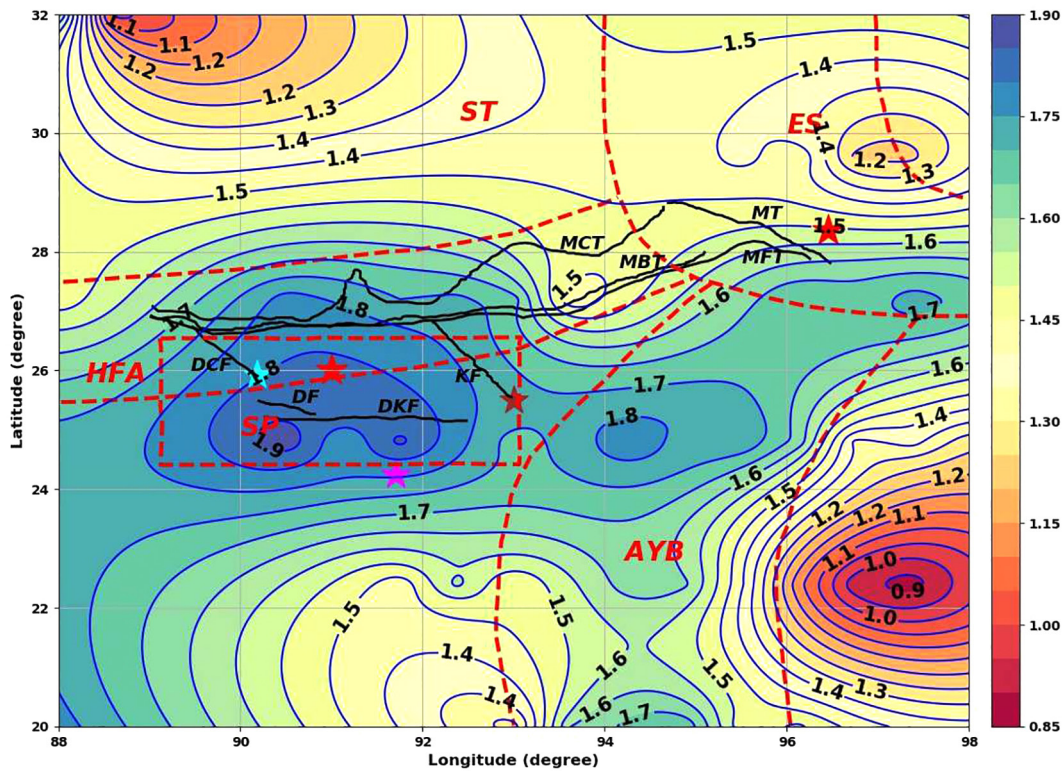


Fig. 8. Spatial fractal dimension (D_c) contour map of the study area. D_c values are plotted for the mean value of longitude and latitude of $2^\circ \times 2^\circ$ square grid with window shifting of 0.5° along the direction of longitude. For detailed explanations and location of the regions see Figure 1.

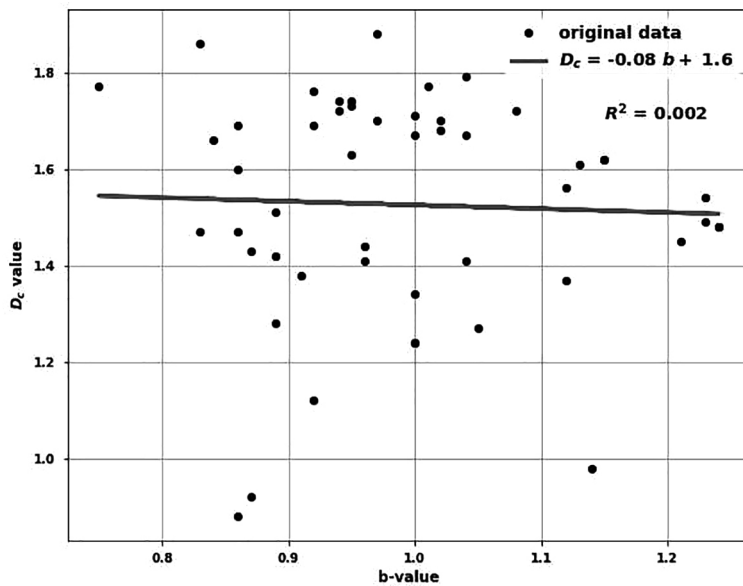


Fig. 9. Correlation between b -value and D_c for the entire study area. The straight line represents the fitted regression line. The b -values and D_c are obtained for $2^\circ \times 2^\circ$ square grid of selected regions. For location of the regions see Figure 1.

5. Conclusions

To assess the level of stress and understand the seismic characteristics of the region between $20\text{--}32^\circ\text{N}$ and $88\text{--}98^\circ\text{E}$, the b -value and fractal correlation dimension (D_c) of seismic event epicentres were estimated. These parameters were obtained for five

different regions by analysing the homogeneous database of 1,347 events ($m_b \geq 4.5$) from January 1964 to May 2020. High D_c (> 1.5), except for the South-Tibet region, and b -values around 1.0 reported for regions considered in the present study suggest a high-stress concentrated locked region that signifies the arbitrary occurrence of mostly strong

earthquakes. The subduction thrust on the Indian plate due to external forces generated by the over-riding Burmese plate may be the cause of the greater stress concentration in the region. Therefore, from the present study, we may conclude that:

The regions selected were identified as seismically active with b-values close to 1.0. Relatively low b-value contours (0.8–0.9) are obtained along the Dhubri-Chungthang Fault (DCF) zone, the Dapsi Fault (DF) zone, the Dauki Fault (DKF) zone and the Kopili Fault (KF) zone. These b-values are attributed to the continuous release of strain energy in the region that was accumulated because of northward drifting of the Indian plate towards the Eurasian landmass.

High D_c indicates that the clustering of earthquakes is over a two-dimensional plane and $D_c = 1.36$ obtained for South-Tibet shows the existence of the active linear fault in the region. Higher D_c contours near the Shillong Plateau are due to the heterogeneous fracture structures along the Dauki, Dapsi and Kopili faults. Likewise, the higher D_c obtained for the Arakan-Yoma belt represents a greater stress concentration because of the interaction between the subducting Indian plate and the super-seding Burmese plate. By indexing the b-value and correlation fractal dimension, the present study improves our understanding of the regional features of seismicity, stress level and crustal heterogeneity.

Software resources

The plots were made using Python, Generic Mapping Tools (Wessel et al., 2013) and ZMAP (Wiemer, 2001).

Acknowledgements

The first author wishes to recognise the Tribhuvan University (Nepal) for providing study leave and the University Grants Commission-UGC (Nepal) for providing financial support in the form of a fellowship. Furthermore, both authors are grateful to two anonymous reviewers for their valuable comments.

References

Aki, K., 1965. Maximum likelihood estimate of b in the formula $\log N = a - bM$ and its confidence limits. *Bulletin of Earthquake Research Institute Tokyo University* 43, 237–239.

- Akol, B. & Bekler, T., 2013. Assessment of the statistical earthquake hazard parameters for NW Turkey. *Natural Hazards* 68, 837–853.
- Angelier, J. & Baruah, S., 2009. Seismotectonics in North-east India: A stress analysis of focal mechanism solutions of earthquakes and its kinematic implications. *Geophysical Journal International* 178, 303–326.
- Aviles, C.A., Scholz, C.H. & Boatwright, J., 1987. Fractal analysis applied to characteristic segments of the San Andreas fault (USA). *Journal of Geophysical Research* 92, 331–344.
- Berthet, T., Ritz, J.F., Ferry, M., Pelgay, P., Cattin, R., Drukpa, D., Braucher, R. & Hetényi, G., 2014. Active tectonics of the eastern Himalaya: New constraints from the first tectonic geomorphology study in southern Bhutan. *Geology* 42, 427–430.
- Bhattacharya, P.M. & Kayal, J.R., 2003. Mapping the b-value and its correlation with the fractal dimension in the northeast region of India. *Journal of the Geological Society of India* 62, 680–695.
- Bhattacharya, P.M., Kayal, J.R., Baruah, S. & Arefiev, S.S., 2010. Earthquake Source Zones in Northeast India: Seismic Tomography, Fractal Dimension and b Value Mapping. *Pure and Applied Geophysics* 167, 999–1012.
- Bilham, R., Mencin, D., Bendick, R. & Bürgmann, R., 2017. Implications for elastic energy storage in the Himalaya from the Gorkha 2015 earthquake and other incomplete ruptures of the Main Himalayan Thrust. *Quaternary International* 462, 3–21.
- Bondár, I. & Storchak, D., 2011. Improved location procedures at the International Seismological Centre. *Geophysical Journal International* 186, 1220–1244.
- Bora, D.K., 2016. Scaling relations of moment magnitude, local magnitude, and duration magnitude for earthquakes originated in northeast India. *Earthquake Science* 29, 153–164.
- Bora, D.K. & Baruah, S., 2012. Mapping the crustal thickness in Shillong-Mikir Hills Plateau and its adjoining region of northeastern India using Moho reflected waves. *Journal of Asian Earth Sciences* 48, 83–92.
- Bora, D.K., Baruah, S., Biswas, R. & Gogoi, N.K., 2013. Estimation of source parameters of local earthquakes originated in Shillong-Mikir plateau and its adjoining region of Northeastern India. *Bulletin of Seismological Society of America* 103, 437–446.
- Bora, D.K., Borah, K., Mahanta, R. & Borgohain, J.M., 2018. Seismic b-values and its correlation with seismic moment and Bouguer gravity anomaly over Indo-Burma ranges of northeast India: Tectonic implications. *Tectonophysics* 728–729, 130–141.
- Bora, D.K., Mukherjee, P., Singh, A.P., Borah, K. & Biswas, R., 2022a. Source parameters and scaling relations for small to moderate earthquakes in the Indo-Burma Ranges, North-east India, and its seismotectonic implications. *Geological Journal* 57, 863–876.
- Bora, D.K., Singh, A.P., Borah, K., Anand, A., Biswas, R. & Mishra, O.P., 2022b. Crustal Structure Beneath the Indo-Burma Ranges from the Teleseismic Receiver Function and Its Implications for Dehydration of the Subducting Indian Slab. *Pure and Applied Geophysics* 179, 197–216.

- Borgohain, J.M., Borah, K., Biswas, R. & Bora, D.K., 2018. Seismic b-value anomalies prior to the 3rd January 2016, Mw = 6.7 Manipur earthquake of northeast India. *Journal of Asian Earth Sciences* 154, 42–48.
- Cao, A. & Gao, S.S., 2002. Temporal variation of seismic b-values beneath northeastern Japan island arc. *Geophysical Research Letters* 29, 481–483.
- Chen, J. & Zhu, S., 2020. Spatial and temporal b-value precursors preceding the 2008 Wenchuan, China, earthquake (Mw = 7.9): implications for earthquake prediction. *Geomatics, Natural Hazards and Risk* 11, 1196–1211.
- Dasgupta, S., Mukhopadhyay, B., Mukhopadhyay, M. & Pande, P., 2021. Geo- and seismo- tectonics of Eastern Himalaya: Exploring earthquake source zones from foredeep to Tibetan hinterland. *Physics and Chemistry of the Earth* 123, 103013.
- Devi, S., Arora, S., Kumar, P. & Yadov, M., 2021. Strong-Motion Simulation of the 1988 Indo-Burma and Scenario Earthquakes in NE India by Integrating Site Effects in a Semi-Empirical Technique. *Pure and Applied Geophysics* 178, 2839–2854.
- Diehl, T., Singer, J., Hetényi, G., Grujic, D., Clinton, J., Giardini, D. & Kissling, E., 2017. Seismotectonics of Bhutan: Evidence for segmentation of the Eastern Himalayas and link to foreland deformation. *Earth and Planetary Science Letters* 471, 54–64.
- El-Isa, Z.H. & Eaton, D.W., 2014. Spatiotemporal variations in the b-value of earthquake magnitude-frequency distributions: Classification and causes. *Tectonophysics* 615–616, 1–11.
- Ghosal, A., Ghosh, U. & Kayal, J.R., 2012. A detailed b-value and fractal dimension study of the March 1999 Chamoli earthquake (Ms 6.6) aftershock sequence in western Himalaya. *Geomatics, Natural Hazards and Risk* 3, 271–278.
- Grassberger, P. & Procaccia, I., 1983. Characterization of strange attractors. *Physical Review Letters* 50, 346–349.
- Gutenberg, B. & Richter, C.F., 1944. Frequency of earthquakes in California. *Bulletin of the Seismological Society of America* 34, 185–188.
- Hirata, T., 1989a. A correlation between the b value and the fractal dimension of earthquakes. *Journal of Geophysical Research* 94, 7507–7514.
- Hirata, T., 1989b. Fractal Dimension of Fault Systems in Japan: Fractal Structure in Rock Fracture Geometry at Various Scales. *Pure and Applied Geophysics* 131, 157–170.
- Ishibe, T., Satake, K., Sakai, S., Shimazaki, K., Tsuruoka, H., Yokota, Y., Nakagawa, S. & Hirata, N., 2015. Correlation between Coulomb stress imparted by the 2011 Tohoku-Oki earthquake and seismicity rate change in Kanto, Japan. *Geophysical Journal International* 201, 112–134.
- Islam, M.S., Shinjo, R. & Kayal, J.R., 2011. Pop-up tectonics of the Shillong Plateau in northeastern India: Insight from numerical simulations. *Gondwana Research* 20, 395–404.
- Kagan, Y. & Knopoff, L., 1978. Statistical study of the occurrence of shallow earthquakes. *Geophysical Journal of the Royal Astronomical Society* 55, 67–86.
- Kayal, J.R., 2010. Himalayan tectonic model and the great earthquakes: An appraisal. *Geomatics, Natural Hazards and Risk* 1, 51–67.
- Kayal, J.R., Arefiev, S.S., Baruah, S., Hazarika, D., Gogoi, N., Gautam, J.L., Baruah, S., Dorbath, C. & Tatevossian, R., 2012. Large and great earthquakes in the Shillong plateau-Assam valley area of Northeast India Region: Pop-up and transverse tectonics. *Tectonophysics* 532–535, 186–192.
- Kayal, J.R., Arefiev, S.S., Baruah, S., Hazarika, D., Gogoi, N., Kumar, A., Chowdhury, S.N. & Kalita, S., 2006. Shillong plateau earthquakes in northeast India region: Complex tectonic model. *Current Science* 91, 109–114.
- Kayal, J.R., Reena, D. & Chakraborty, P.P., 1993. Microearthquakes at the main boundary thrust in Eastern Himalaya and the present-day tectonic model. *Tectonophysics* 218, 375–381.
- Khan, P.K. & Chakraborty, P.P., 2007. The seismic b-value and its correlation with Bouguer gravity anomaly over the Shillong Plateau area: Tectonic implications. *Journal of Asian Earth Sciences* 29, 136–147.
- Khan, P.K., Ghosh, M., Chakraborty, P.P. & Mukherjee, D., 2011. Seismic b-Value and the assessment of ambient stress in Northeast India. *Pure and Applied Geophysics* 168, 1693–1706.
- Khattari, K.M. & Tyagi, A.K., 1983. Seismicity patterns in the Himalayan plate boundary and identification of the areas of high seismic potential. *Tectonophysics* 96, 281–297.
- Kumar, S. & Sharma, N., 2019. The seismicity of central and north-east Himalayan region. *Contributions to Geophysics and Geodesy* 49, 265–281.
- Legrand, D., 2002. Fractal dimensions of small, intermediate, and large earthquakes. *Bulletin of the Seismological Society of America* 92, 3318–3320.
- Liu, J., Ji, C., Zhang, J., Zhang, P., Zeng, L., Li, Z. & Wang, W., 2015. Tectonic setting and general features of coseismic rupture of the 25 April, 2015 Mw 7.8 Gorkha, Nepal earthquake. *Kexue Tongbao/Chinese Science Bulletin* 60, 2640–2658.
- Mandelbrot, B.B. & Wheeler, J.A., 1983. The Fractal Geometry of Nature. *American Journal of Physics* 51, 286–287.
- Mogi, K., 1967. Earthquakes and fractures. *Tectonophysics* 5, 35–55.
- Molnar, P. & Tapponnier, P., 1975. Cenozoic tectonics of Asia: Effects of a continental collision. *Science* 189, 419–426.
- Mondal, S.K., Roy, P.N.S., Catherine, J.K. & Pandey, A.K., 2019. Significance of fractal correlation dimension and seismic b-value variation due to 15th July 2009, New Zealand earthquake of mw 7.8. *Annals of Geophysics* 62, 1–17.
- Mousavi, S.M., 2017a. Mapping seismic moment and b-value within the continental-collision orogenic-belt region of the Iranian Plateau. *Journal of Geodynamics* 103, 26–41.
- Mousavi, S.M., 2017b. Spatial variation in the frequency-magnitude distribution of earthquakes under the tectonic framework in the Middle East. *Journal of Asian Earth Sciences* 147, 193–209.

- Nandy, D.R., 2005. Geodynamics and Seismicity of Northeast India and its Adjoining areas. *Special Publication Geological Survey of India* 85, 49–59.
- Nandy, D.R. & Dasgupta, S., 1991. Seismotectonic Domains of Northeastern India and Adjacent areas. *Physics and Chemistry of the Earth* 18, 371–384.
- Nava, F.A., Márquez-Ramírez, V.H., Zúñiga, F.R. & Lomnitz, C., 2017. Gutenberg–Richter b-value determination and large-magnitudes sampling. *Natural Hazards* 87, 1–11.
- Nerenberg, M.A.H. & Essex, C., 1990. Correlation dimension and systematic geometric effects. *Physical Review A* 42, 7065–7074.
- Oncel, A.O. & Wilson, T., 2002. Space-time correlations of seismotectonic parameters: Examples from Japan and from Turkey preceding the İzmit earthquake. *Bulletin of the Seismological Society of America* 92, 339–349.
- Oncel, A.O. & Wilson, T., 2007. Anomalous seismicity preceding the 1999 İzmit event, NW Turkey. *Geophysical Journal International* 169, 259–270.
- Öncel, A.O., Alptekin, Ö. & Main, I., 1995. Temporal variations of the fractal properties of seismicity in the western part of the north anatolian fault zone: Possible artifacts due to improvements in station coverage. *Nonlinear Processes in Geophysics* 2, 147–157.
- Öncel, A.O., Main, I., Alptekin, Ö. & Cowie, P., 1996. Spatial variations of the fractal properties of seismicity in the Anatolian fault zones. *Tectonophysics* 257, 189–202.
- Pailoplee, S. & Choowong, M., 2014. Earthquake frequency-magnitude distribution and fractal dimension in mainland Southeast Asia. *Earth, Planets and Space* 66, 1–10.
- Panthi, A., Singh, H.N. & Shanker, D., 2013. Revisiting State of Stress and Geodynamic Processes in North-east India Himalaya and Its Adjoining Region. *Geosciences* 3, 143–152.
- Pudi, R., Martha, T.R., Kumar, K.V., Ramesh, P., Martha, T.R. & Kumar, K.V., 2020. Regional variation of stress level in the Himalayas after the 25 April 2015 Gorkha earthquake (Nepal) estimated using b-values. *Journal of Geophysics and Engineering* 15, 921–927.
- Raghu Kanth, S.T.G. & Dash, S.K., 2010. Deterministic seismic scenarios for North East India. *Journal of Seismology* 14, 143–167.
- Reasenber, P., 1985. Second-order moment of central California seismicity, 1969–1982. *Journal of Geophysical Research: Solid Earth* 90, 5479–5495.
- Roy, P.N.S. & Padhi, A., 2007. Multifractal analysis of earthquakes in the Southeastern Iran-Bam Region. *Pure and Applied Geophysics* 164, 2271–2290.
- Roy, P.N.S., Chowdhury, S., Sarkar, P. & Mondal, S.K., 2015. Fractal study of seismicity in order to characterize the various tectonic blocks of North-east Himalaya, India. *Natural Hazards* 77, S5–S18.
- Sarkar, P., Roy, P.N.S. & Pal, S.K., 2020. Rejuvenation of ‘pop-up’ tectonics for Shillong Plateau in NE Himalayan region. *Journal of Earth System Science* 129, 123.
- Scholz, C.H., 1968. The frequency-magnitude relation of microfracturing in rock and its relation to earthquakes. *Bulletin of the Seismological Society of America* 58, 399–415.
- Scholz, C.H., 2015. On the stress dependence of the earthquake b value. *Geophysical Research Letters* 42, 1399–1402.
- Shi, Y. & Bolt, A.B., 1982. The standard error of the magnitude-frequency b value. *Bulletin of the Seismological Society of America* 72, 1677–1687.
- Singh, C., Singh, A. & Chadha, R.K., 2009. Fractal and b-value mapping in eastern Himalaya and southern Tibet. *Bulletin of the Seismological Society of America* 99, 3529–3533.
- Storchak, D.A., Harris, J., Brown, L., Lieser, K., Shumba, B. & Di Giacomo, D., 2020. Rebuild of the Bulletin of the International Seismological Centre (ISC) – part 2: 1980–2010. *Geoscience Letters* 7, 1980–2010.
- Storchak, D.A., Harris, J., Brown, L., Lieser, K., Shumba, B., Verney, R., Di Giacomo, D. & Korger, E.I.M., 2017. Rebuild of the Bulletin of the International Seismological Centre (ISC). *Geoscience Letters* 4, 1964–1979.
- Tandon, S.K. & Gupta, N., 2020. Introduction to geodynamics of the indian plate: Evolutionary perspectives. In: N. Gupta & S. Tandon (Eds): *Geodynamics of the Indian Plate*. Springer Geology. Springer, Cham. https://doi.org/10.1007/978-3-030-15989-4_1
- Thingbaijam, K.K.S., Nath, S.K., Yadav, A., Raj, A., Walling, M.Y. & Mohanty, W.K., 2008. Recent seismicity in Northeast India and its adjoining region. *Journal of Seismology* 12, 107–123.
- Tosi, P., 1998. Seismogenic structure behaviour revealed by spatial clustering of seismicity in the Umbria-Marche Region (Central Italy). *Annals of Geophysics* 41, 215–224.
- Turcotte, D.L., 1989. Fractals in geology and Geophysics. *Pure and Applied Geophysics* 131, 171–196.
- Verma, R.K., Mukhopadhyay, M. & Ahluwalia, M.S., 1976. Earthquake mechanisms and tectonic features of Northern Burma. *Tectonophysics* 32, 387–399.
- Wessel, P., Smith, W.H.F., Scharroo, R., Luis, J. & Wobbe, F., 2013. Generic mapping tools: Improved version released. *Eos* 94, 409–410.
- Wiemer, S., 2001. A software package to analyze seismicity: ZMAP. *Seismological Research Letters* 72, 373–382.
- Wiemer, S. & Wyss, M., 1997. Mapping the frequency-magnitude distribution in asperities: An improved technique to calculate recurrence times? *Journal of Geophysical Research: Solid Earth* 102, 15115–15128.
- Wiemer, S. & Wyss, M., 2000. Minimum magnitude of completeness in earthquake catalogs: Examples from Alaska, the Western United States, and Japan. *Bulletin of the Seismological Society of America* 90, 859–869.
- Woessner, J., 2005. Assessing the Quality of Earthquake Catalogues: Estimating the Magnitude of Completeness and Its Uncertainty. *Bulletin of the Seismological Society of America* 95, 684–698.
- Wu, H.Y., Liu, H.F., Xu, W.J. & Wang, X., 2017. Fractal dimension and b value of the aftershock sequence of the 2008 Ms 8.0 wenchuan earthquake. *Natural Hazards* 88, 315–325.
- Wyss, M., Sammis, C.G., Nadeau, R.M. & Wiemer, S., 2004. Fractal dimension and b-value on creeping and locked patches of the San Andreas fault near Park-

- field, California. *Bulletin of the Seismological Society of America* 94, 410-421.
- Yadav, R.B.S., Tripathi, J.N., Shanker, D., Rastogi, B.K., Das, M.C. & Kumar, V., 2011. Probabilities for the occurrences of medium to large earthquakes in north-east India and adjoining region. *Natural Hazards* 56, 145-167.
- Zhang, J., Santosh, M., Wang, X., Guo, L., Yang, X. & Zhang, B., 2012. Tectonics of the northern Himalaya since the India-Asia collision. *Gondwana Research* 21, 939-960.
- Zhao, Y.Z. & Wu, Z.L., 2008. Mapping the ν -values along the Longmenshan fault zone before and after the 12 May 2008, Wenchuan, China, MS 8.0 earthquake. *Natural Hazards and Earth System Sciences* 8, 1375-1385.

Manuscript submitted: 23 March 2022

Revision accepted: 19 July 2022